Proceedings of the 40th Chinese Control Conference
July 26-28, 2021, Shanghai, China

Control of an Underactuated Reusable Launch Vehicle by Partial Feedback Linearization

Linqi Ye [1], Jiayi Li [2], Changliang Wang[3], Houde Liu[4], Bin Liang[5]

1. The Center of Intelligent Control and Telescience, Tsinghua Shenzhen International Graduate School, Tsinghua University, Shenzhen 518055, China
E-mail: ye.linqi@sz.tsinghua.edu.cn

2.School of Mechanical Engineering and Automation, Harbin Institute of Technology, Shenzhen, Shenzhen 518055, China
E-mail: lijiayi@stu.hit.edu.cn

3.Shanghai Academy of Spaceflight Technology, Shanghai 201109, China
E-mail: sastty@163.com

4. The Center of Intelligent Control and Telescience, Tsinghua Shenzhen International Graduate School, Tsinghua University, Shenzhen 518055, China
E-mail:liu.hd@sz.tsinghua.edu.cn

5. Navigation and Control Research Center, Department of Automation, Tsinghua University, Beijing 100084, China
E-mail:bliang@tsinghua.edu.cn

Abstract: The control issue of an underactuated reusable launch vehicle (RLV) involving nonminimum phase problem is considered in this paper. The considered RLV system has more outputs than the available inputs, preventing it from fully feedback linearization by traditional dynamic inversion or backstepping methods. To address this issue, an approach combining backstepping and partial feedback linearization is proposed, which linearizes the system to the maximum extent and locally stabilize the nonlinear part at the same time. The controller is divided into an outer loop which is the attitude angle subsystem and an inner loop which is the angular rate subsystem. The outer loop controller is designed like standard backstepping while the inner loop uses a partial feedback linearization control law to stabilize the system with limited numbers of control inputs. A disturbance observer is designed for each loop to estimate the lumped uncertainties and the estimation is incorporated into the controller to make the control system more robust. Stability analysis are given, and numerical simulations are taken to validate the effectiveness of the proposed method.

Key Words: reusable launch vehicle (RLV), underactuated system, nonminimum phase problem, backstepping, partial feedback linearization

1 Introduction

Launch vehicle system is an important technology which can send human and payload into earth orbit as well as outer space. In the past decades, scientists are making great efforts to lower down the cost of each launch, leading to the birth of a new technology, reusable launch vehicles (RLVs). An RLV is usually launched into orbit by a rocket and will return into atmosphere for the next use. From the space shuttle to the X-33 spaceplane, the crew return vehicle X-38, and the recent Falcon heavy rocket, reusable launch vehicles have shown great potential to provide an economic way to enter space in the future.

The RLV dynamics are characterized by high nonlinearities, strong couplings, fast time-varying, and great uncertainties, making it a challenging task to design control systems for this kind of vehicles. During the reentry phase, RLV flies like a glider which has poor maneuverability, in which its attitude is controlled by aerodynamic surfaces and a reaction control system (RCS). In recent years, several nonlinear control methods have been proposed for the attitude control of RLVs. In [1-3], the sliding mode control method, including a high-order sliding mode, a nonsingular sliding mode, and a super-twisting sliding mode controller are applied to control RLVs. In [4-6], backstepping control has shown good capability to handle the complicated RLV dynamics. In [7-9], the disturbance observer technique is employed together with the nonlinear control methods to make the controller more robust against model uncertainties and disturbances. Besides, fuzzy control is proposed in [10] and neural network control is developed in [11] for RLVs, which can identify the system model and doesn't rely on exact model knowledge.

The realistic reentry control of an RLV is very complicated due to the large flight envelope, during which its flight speed and dynamic pressure suffer from great changes from the beginning to the end of reentry. A practical issue is the nonminimum phase problem caused by underactuation during the middle phase of reentry. Take X-38 as an example, there is a significant portion when the dynamic pressure is greater than 1500 and the Mach number is more than 6, during which the vehicle is underactuated since the RCS thrusters are no longer available and the rudders are not yet been used [12-14]. During this period, X-38 has more outputs than the available inputs. That is, the attack angle, sideslip angle, and bank angle are controlled by only two body flaps. Therefore, the aforementioned methods are no longer available since they assume that the moments about all three body axes are available.

*This work is supported by National Natural Science Foundation (NNSF) of China under Grant 62003188, 61803221, 11702176 and U1813216.

For an underactuated RLV, the control challenge lies in the nonminimum phase problem. As shown in [14-15], the sideslip angle dynamics of an underactuated RLV exhibit nonminimum phase behaviour and will cause unsatisfactory oscillations or divergence if not properly treated. Therefore, new control methods are required to address the nonminimum phase problem for an underactuated RLV system. To date, only several results are given in literature for this problem, including an output redefinition method [14], a dynamic sliding mode approach [15] and an output feedback controller that combines output redefinition and extended state observer [16].

In this paper, a new method is developed to address the underactuated RLV control problem by using partial feedback linearization. For underactuated systems that cannot be fully linearized through feedback, partial feedback linearization can serve as an alternative to design a controller and has been applied to several underactuated systems such as a legged robot [17], a crane system [18], and a photovoltaic system [19], just name a few. The key idea of partial feedback linearization is to linearize the underactuated system to the maximum extent and stabilize the nonlinear part by proper use of the coupling effect. Like feedback linearization, partial feedback linearization is usually carried out with dynamic inversion. However, for an underactuated RLV system, its attitude dynamics are complicated and not in an integral chain form, making it inconvenient to implement dynamic inversion. Therefore, we take advantage of backstepping control [20] to design the control law in a recursive way, which is very suitable for the underactuated RLV system that is in a strict-feedback form. The controller is divided into an outer loop which is the attitude angle subsystem and an inner loop which is the angular rate subsystem. The outer loop controller is designed by standard backstepping. For the inner loop, a partial feedback linearization control law is designed to stabilize the system by using fewer inputs. Besides, a disturbance observer is designed for each loop to estimate the lumped uncertainties and the estimate is incorporated into the controller to make the control system more robust. Stability analysis are given to prove the theoretical stability and numerical simulations are taken to further validate the effectiveness of the proposed method.

The contributions of this paper are twofold. First, a systematic way is proposed to solve the nonminimum phase problem of an underactuated RLV by using partial feedback linearization. The proposed method is simpler compared to the existed methods [14-16] since it only requires a small modification on the methods designed for a fully actuated RLV. Second, the combination of backstepping with partial feedback linearization is proved very effective for underactuated systems which are not in an integral chain form and may be applied to other underactuated systems in the future.

The outline of this paper is as follows. First, the underactuated RLV model is introduced in Section 2. Controller design is shown in Section 3 and simulations are given in Section 4. Finally, conclusions are given in Section 5.

2 Underactuated RLV Model

The considered underactuated RLV model is based on the X-38 crew return vehicle. We will focus on the underactuated period when the system has only two control inputs available. The total deflection and differential deflection of the two body flaps form the two control inputs, i.e., the elevator deflection δ_e and the aileron deflection δ_a. Following [16-17], the attitude dynamics of an underactuated RLV are written as follow:

$$
\begin{aligned}
\dot{\alpha} &= -p\cos\alpha\tan\beta + q - r\sin\alpha\tan\beta + \frac{g_0}{V_0\cos\beta}\cos\mu\cos\gamma_0 \\
&\quad - \frac{L}{m_0 V_0\cos\beta} \\
\dot{\beta} &= p\sin\alpha - r\cos\alpha + \frac{g_0}{V_0}\sin\mu\cos\gamma_0 - \frac{Y}{m_0 V_0} \\
\dot{\mu} &= p\cos\alpha\frac{1}{\cos\beta} + r\sin\alpha\frac{1}{\cos\beta} + \frac{L\tan\beta}{m_0 V_0} \\
&\quad - \frac{g_0\tan\beta}{V_0}\cos\mu\cos\gamma_0 + \frac{\tan\gamma_0}{m_0 V_0}\left(-Y\cos\mu + L\sin\mu\right) \\
\dot{p} &= \frac{I_{xz}\left(I_x - I_y + I_z\right)pq + \left(I_y I_z - I_z^2 - I_{xz}^2\right)qr}{I_x I_z - I_{xz}^2} + L'_\beta\beta + L'_{\delta_a}\delta_a \\
\dot{q} &= \frac{\left(I_z - I_x\right)pr + I_{xz}\left(r^2 - p^2\right)}{I_y} + M'_\alpha\Delta\alpha + M'_{\delta_e}\Delta\delta_e \\
\dot{r} &= \frac{I_{xz}\left(-I_x + I_y - I_z\right)qr + \left(I_x^2 - I_x I_y + I_{xz}^2\right)pq}{I_x I_z - I_{xz}^2} + N'_\beta\beta + N'_{\delta_a}\delta_a
\end{aligned}
\tag{1}
$$

where α, β and μ are the angles of attack, sideslip and bank, respectively, p, q and r are the angular rates of roll, pitch and yaw, respectively. $\Delta\alpha = \alpha - \alpha_T$ and $\Delta\delta_e = \delta_e - \delta_{eT}$ are the deviations of α and δ_e from their trim values. I_x, I_y, and I_z are the moments of inertia about the three body axes. m_0 and g_0 are vehicle mass and gravitational acceleration, respectively. V_0 and γ_0 are flight path velocity and flight path angle, respectively. L and Y represent lift and side force, respectively. L'_β, L'_{δ_a}, N'_β, N'_{δ_a}, M'_α, and M'_{δ_e} are aerodynamic parameters.

For the convenience of controller design, the model can be rewritten in a strict-feedback form. Denoting $\boldsymbol{\Theta} = [\alpha, \beta, \mu]^T$, $\boldsymbol{\omega} = [p, q, r]^T$ and $\boldsymbol{u} = [\delta_e, \delta_a]^T$, then the control-oriented model is written as follows

$$
\begin{aligned}
\dot{\boldsymbol{\Theta}} &= \boldsymbol{F}_\Theta + \boldsymbol{G}_\Theta\boldsymbol{\omega} + \boldsymbol{d}_\Theta \\
\dot{\boldsymbol{\omega}} &= \boldsymbol{F}_\omega + \boldsymbol{G}_\omega\boldsymbol{u} + \boldsymbol{d}_\omega
\end{aligned}
\tag{2}
$$

where

$$\boldsymbol{F}_{\Theta}= \begin{bmatrix} \dfrac{g_0}{V_0\cos\beta}\cos\mu\cos\gamma_0-\dfrac{L}{m_0V_0\cos\beta} \\ \dfrac{g_0}{V_0}\sin\mu\cos\gamma_0-\dfrac{Y}{m_0V_0} \\ \dfrac{\left(L-m_0g_0\cos\mu\cos\gamma_0\right)\tan\beta+\left(L\sin\mu-Y\cos\mu\right)\tan\gamma_0}{m_0V_0} \end{bmatrix} \tag{3}$$

$$\boldsymbol{G}_{\Theta}=\begin{bmatrix} -\cos\alpha\tan\beta & 1 & -\sin\alpha\tan\beta \\ \sin\alpha & 0 & -\cos\alpha \\ \cos\alpha/\cos\beta & 0 & \sin\alpha/\cos\beta \end{bmatrix}$$

$$\boldsymbol{F}_{\omega}=\begin{bmatrix} \dfrac{I_{xz}\left(I_x-I_y+I_z\right)pq+\left(I_yI_z-I_z^2-I_{xz}^2\right)qr}{I_xI_z-I_{xz}^2}+L_{\beta}^{'}\beta \\ \dfrac{\left(I_z-I_x\right)pr+I_{xz}\left(r^2-p^2\right)}{I_y}+M_{\alpha}^{'}\Delta\alpha-M_{\delta_e}^{'}\delta_{eT} \\ \dfrac{I_{xz}\left(-I_x+I_y-I_z\right)qr+\left(I_x^2-I_xI_y+I_{xz}^2\right)pq}{I_xI_z-I_{xz}^2}+N_{\beta}^{'}\beta \end{bmatrix} \tag{4}$$

$$\boldsymbol{G}_{\omega}=\begin{bmatrix} 0 & L_{\delta_a}^{'} \\ M_{\delta_e}^{'} & 0 \\ 0 & N_{\delta_a}^{'} \end{bmatrix}$$

In this model, $\boldsymbol{d}_{\Theta}$ and $\boldsymbol{d}_{\omega}$ are lumped uncertainties caused by model simplifications and model uncertainties. The controller will be designed based on this model. During reentry, the sideslip angle should be kept near zero to prevent excessive heat buildup, while the attack angle α and bank angle μ are usually required to track some precomputed trajectories. Therefore, the control objective is to track the attack angle profile α_d and the bank angle profile μ_d, while keeping the sideslip angle β close to zero.

3 Partial Feedback Linearization Controller Design

In this section, the controller design will be given by using backstepping and partial feedback linearization. Then stability analysis is derived to show the stability of the closed-loop system.

3.1 Controller Design

Denote $\Theta_d=\left[\alpha_d,0,\mu_d\right]^T$ as the reference profile for the attitude angles and define $\tilde{\Theta}=\Theta-\Theta_d$ as the tracking error. Then the attitude angle error dynamics become

$$\dot{\tilde{\Theta}}=\boldsymbol{F}_{\Theta}+\boldsymbol{G}_{\Theta}\boldsymbol{\omega}+\boldsymbol{d}_{\Theta} \tag{5}$$

where $-\dot{\Theta}_d$ is incorporated into the lumped uncertainty $\boldsymbol{d}_{\Theta}$. Take $\boldsymbol{\omega}$ as the virtual control input and design the desired control law as

$$\boldsymbol{\omega}_d=\boldsymbol{G}_{\Theta}^{-1}\left(k_{\Theta}\tilde{\Theta}-\boldsymbol{F}_{\Theta}-\hat{\boldsymbol{d}}_{\Theta}\right) \tag{6}$$

where $k_{\Theta}>0$ and $\hat{\boldsymbol{d}}_{\Theta}$ is an estimate for the disturbance $\boldsymbol{d}_{\Theta}$ which is obtained by the disturbance observer as follows

$$\begin{aligned} \hat{\boldsymbol{d}}_{\Theta}&=\lambda_{\Theta}\left(\tilde{\Theta}-\xi_{\Theta}\right) \\ \dot{\xi}_{\Theta}&=\boldsymbol{F}_{\Theta}+\boldsymbol{G}_{\Theta}\boldsymbol{\omega}+\hat{\boldsymbol{d}}_{\Theta} \end{aligned} \tag{7}$$

where $\lambda_{\Theta}>0$. Denote $\tilde{\boldsymbol{\omega}}=\boldsymbol{\omega}-\boldsymbol{\omega}_d$ and $\tilde{\boldsymbol{d}}_{\Theta}=\boldsymbol{d}_{\Theta}-\hat{\boldsymbol{d}}_{\Theta}$. Substituting (6) into (5) yields

$$\dot{\tilde{\Theta}}=-k_{\Theta}\tilde{\Theta}+\boldsymbol{G}_{\Theta}\tilde{\boldsymbol{\omega}}+\tilde{\boldsymbol{d}}_{\Theta} \tag{8}$$

Next, consider the angular rate error dynamics

$$\dot{\tilde{\boldsymbol{\omega}}}=\boldsymbol{F}_{\omega}+\boldsymbol{G}_{\omega}\boldsymbol{u}+\boldsymbol{d}_{\omega} \tag{9}$$

where $-\dot{\boldsymbol{\omega}}_d$ is incorporated into the lumped uncertainty $\boldsymbol{d}_{\omega}$. Note that $\tilde{\boldsymbol{\omega}}=\left[\tilde{p},\tilde{q},\tilde{r}\right]^T$ is three-dimensional while $\boldsymbol{u}=\left[\delta_e,\delta_a\right]^T$ is only two-dimensional, indicating that this subsystem cannot be fully linearized through feedback. Therefore, a partial feedback linearization control law will be designed to stabilize this subsystem. For the three variables in $\tilde{\boldsymbol{\omega}}$, two of them can be linearized while the third will remain in a nonlinear form. As one choice but not the only, the dynamics of $\tilde{q}$ and $\tilde{r}$ are selected to be linearized. Denote $\boldsymbol{\varpi}=\left[\tilde{q},\tilde{r}\right]^T$. The dynamics (9) can be divided into two parts, with each of the matrices $\boldsymbol{F}_{\omega}$, $\boldsymbol{G}_{\omega}$, and $\boldsymbol{d}_{\omega}$ decomposed as follows

$$\boldsymbol{F}_{\omega}=\begin{bmatrix} f_p \\ \boldsymbol{F}_{\varpi}\end{bmatrix},\boldsymbol{G}_{\omega}=\begin{bmatrix} \boldsymbol{G}_p \\ \boldsymbol{G}_{\varpi}\end{bmatrix},\boldsymbol{d}_{\omega}=\begin{bmatrix} d_p \\ \boldsymbol{d}_{\varpi}\end{bmatrix} \tag{10}$$

where f_p and $\boldsymbol{F}_{\varpi}$ are defined as the first row and the last two rows of $\boldsymbol{F}_{\omega}$, respectively; $\boldsymbol{G}_p$ and $\boldsymbol{G}_{\varpi}$ represent the first row and the last two rows of $\boldsymbol{G}_{\omega}$, respectively; d_p and $\boldsymbol{d}_{\varpi}$ are the first row and the last two rows of $\boldsymbol{d}_{\omega}$, respectively. Then the dynamics (9) can be rewritten as follows

$$\begin{aligned} \dot{\tilde{p}}&=f_p+\boldsymbol{G}_p\boldsymbol{u}+d_p \\ \dot{\boldsymbol{\varpi}}&=\boldsymbol{F}_{\varpi}+\boldsymbol{G}_{\varpi}\boldsymbol{u}+\boldsymbol{d}_{\varpi} \end{aligned} \tag{11}$$

Define a partial feedback linearization transformation as follows

$$\boldsymbol{u}=\boldsymbol{G}_{\varpi}^{-1}\left(\boldsymbol{v}-\boldsymbol{F}_{\varpi}-\hat{\boldsymbol{d}}_{\varpi}\right) \tag{12}$$

where $\boldsymbol{v}$ is the transformed control input and $\hat{\boldsymbol{d}}_{\varpi}$ is an estimate for the disturbance $\boldsymbol{d}_{\varpi}$ which is obtained by the disturbance observer as follows

$$\begin{aligned} \hat{\boldsymbol{d}}_{\varpi}&=\lambda_{\varpi}\left(\boldsymbol{\varpi}-\xi_{\varpi}\right) \\ \dot{\xi}_{\varpi}&=\boldsymbol{F}_{\varpi}+\boldsymbol{G}_{\varpi}\boldsymbol{\omega}+\hat{\boldsymbol{d}}_{\varpi} \end{aligned} \tag{13}$$

where $\lambda_{\varpi}>0$. Denote $\tilde{\boldsymbol{d}}_{\varpi}=\boldsymbol{d}_{\varpi}-\hat{\boldsymbol{d}}_{\varpi}$. Substituting (12) into (11) yields

$$\begin{aligned} \dot{\tilde{p}}&=f_p+\boldsymbol{G}_p\boldsymbol{G}_{\varpi}^{-1}\left(\boldsymbol{v}-\boldsymbol{F}_{\varpi}-\hat{\boldsymbol{d}}_{\varpi}\right)+d_p \\ \dot{\boldsymbol{\varpi}}&=\boldsymbol{v}+\tilde{\boldsymbol{d}}_{\varpi} \end{aligned} \tag{14}$$

According to the definition, it is known that $\boldsymbol{G}_p\boldsymbol{G}_{\varpi}^{-1}=\left[0 \quad L_{\delta_a}^{'}/N_{\delta_a}^{'}\right]$. Therefore, system (14) can be written as follows

$$\begin{bmatrix} \dot{\tilde{p}} \\ \dot{\tilde{q}} \\ \dot{\tilde{r}} \end{bmatrix}=\begin{bmatrix} 0 & L_{\delta_a}^{'}/N_{\delta_a}^{'} \\ 1 & 1 \\ 1 & 1 \end{bmatrix}\boldsymbol{v}+\boldsymbol{d} \tag{15}$$

where

$$\boldsymbol{d} = \begin{bmatrix} f_p + \boldsymbol{G}_p \boldsymbol{G}_{\varpi}^{-1}\left(-\boldsymbol{F}_{\varpi} - \hat{\boldsymbol{d}}_{\varpi}\right) + d_p \\ \tilde{\boldsymbol{d}}_{\varpi} \end{bmatrix} \tag{16}$$

Design the control law as follows

$$\boldsymbol{v} = \begin{bmatrix} k_{11}\tilde{p} + k_{12}\tilde{q} + k_{13}\tilde{r} \\ k_{21}\tilde{p} + k_{22}\tilde{q} + k_{23}\tilde{r} \end{bmatrix} \tag{17}$$

where $k_{11}, k_{12}, k_{13}, k_{21}, k_{22}, k_{23}$ are parameters to be designed. Substituting (17) into (16) gives

$$\begin{bmatrix} \dot{\tilde{p}} \\ \dot{\tilde{q}} \\ \dot{\tilde{r}} \end{bmatrix} = \begin{bmatrix} k_{21}L'_{\delta_a} / N'_{\delta_a} & k_{22}L'_{\delta_a} / N'_{\delta_a} & k_{23}L'_{\delta_a} / N'_{\delta_a} \\ k_{11} & k_{12} & k_{13} \\ k_{21} & k_{22} & k_{23} \end{bmatrix} \begin{bmatrix} \tilde{p} \\ \tilde{q} \\ \tilde{r} \end{bmatrix} + \boldsymbol{d} \tag{18}$$

It should be noted that $\boldsymbol{d}$ only contains one nonlinear element in the first line according to (16). Therefore, the overall system is partially linearized with the proposed controller and the nonlinear item in the closed-loop system is treated as a disturbance.

3.2 Stability Analysis

First, stability analysis will be taken on the disturbance observer. It is assumed that $\boldsymbol{d}_\Theta$ and $\boldsymbol{d}_\varpi$ are slow varying disturbances so that $\dot{\boldsymbol{d}}_\Theta \approx \boldsymbol{0}$ and $\dot{\boldsymbol{d}}_\varpi \approx \boldsymbol{0}$. Differentiating $\tilde{\boldsymbol{d}}_\Theta = \boldsymbol{d}_\Theta - \hat{\boldsymbol{d}}_\Theta$ along (7) follows

$$\begin{aligned} \dot{\tilde{\boldsymbol{d}}}_\Theta &= -\dot{\hat{\boldsymbol{d}}}_\Theta = -\lambda_\Theta\left(\dot{\tilde{\Theta}} - \dot{\xi}_\Theta\right) \\ &= -\lambda_\Theta\left[\left(\boldsymbol{F}_\Theta + \boldsymbol{G}_\Theta\boldsymbol{\omega} + \boldsymbol{d}_\Theta\right) - \left(\boldsymbol{F}_\Theta + \boldsymbol{G}_\Theta\boldsymbol{\omega} + \hat{\boldsymbol{d}}_\Theta\right)\right] \\ &= -\lambda_\Theta\tilde{\boldsymbol{d}}_\Theta \end{aligned} \tag{19}$$

Similarly, differentiating $\tilde{\boldsymbol{d}}_\varpi = \boldsymbol{d}_\varpi - \hat{\boldsymbol{d}}_\varpi$ along (13) follows

$$\begin{aligned} \dot{\tilde{\boldsymbol{d}}}_\varpi &= -\dot{\hat{\boldsymbol{d}}}_\varpi = -\lambda_\varpi\left(\dot{\boldsymbol{\varpi}} - \dot{\xi}_\varpi\right) \\ &= -\lambda_\varpi\left[\left(\boldsymbol{F}_\varpi + \boldsymbol{G}_\varpi\boldsymbol{u} + \boldsymbol{d}_\varpi\right) - \left(\boldsymbol{F}_\varpi + \boldsymbol{G}_\varpi\boldsymbol{\omega} + \hat{\boldsymbol{d}}_\varpi\right)\right] \\ &= -\lambda_\varpi\tilde{\boldsymbol{d}}_\varpi \end{aligned} \tag{20}$$

So $\tilde{\boldsymbol{d}}_\Theta$ and $\tilde{\boldsymbol{d}}_\varpi$ will converge to zero asymptotically.

Now turn to the stability analysis for the closed-loop system. For the angular rate subsystem (18), the square matrix on the right hand side can be made asymptotically stable by selecting proper values for $k_{11}, k_{12}, k_{13}, k_{21}, k_{22}, k_{23}$. Furthermore, by assuming $\boldsymbol{d}$ be a bounded disturbance, it can be concluded that system (18) is bounded stable. Therefore, $\tilde{\boldsymbol{\omega}} = \left[\tilde{p}, \tilde{q}, \tilde{r}\right]^T$ will converge to a small region around zero with proper control parameters.

For the attitude angle subsystem (8), it is input-to-state stable from $\boldsymbol{G}_\Theta\tilde{\boldsymbol{\omega}} + \tilde{\boldsymbol{d}}_\Theta$ to $\tilde{\boldsymbol{\Theta}}$. As shown in the previous, both $\tilde{\boldsymbol{\omega}}$ and $\tilde{\boldsymbol{d}}_\Theta$ are bounded, plus assume $\boldsymbol{G}_\Theta$ is bounded so that $\boldsymbol{G}_\Theta\tilde{\boldsymbol{\omega}} + \tilde{\boldsymbol{d}}_\Theta$ is bounded as a whole, which indicates that $\tilde{\boldsymbol{\Theta}}$ is bounded according to the Input-to-State Stability Theorem [20]. Therefore, by choosing the control gain k_Θ properly, the attitude angle tracking error $\tilde{\boldsymbol{\Theta}}$ will converge to a small region around zero. This completes the proof.

4 Simulations

Numerical simulation results are shown in this section to validate the effectiveness of the proposed method. The nominal model parameters are listed in Table 1 and the control parameters in Table 2.

Table 1: Nominal values of the model parameters

Parameter	Definition	Value	Parameter	Definition	Value
m_0	Vehicle mass	68.5	α_T	Trim angle of attack	0.66
V_0	Flight path velocity	17192	δ_{eT}	Trim elevator deflection	0.17
g_0	Gravitational acceleration	32.2	L'_β	Aerodynamic parameter	–25.1
γ_0	Flight path angle	0	L'_{δ_a}	Aerodynamic parameter	–10.6
I_x	Moment of inertia about x body axis	203.4	N'_β	Aerodynamic parameter	–1.53
I_y	Moment of inertia about y body axis	1356	N'_{δ_a}	Aerodynamic parameter	0.53
I_z	Moment of inertia about z body axis	1627	M'_α	Aerodynamic parameter	10.0
I_{xz}	Cross product of inertia	27.1	M'_{δ_e}	Aerodynamic parameter	15.1

Table 2: Controller parameters

Parameter	Value	Parameter	Value
k_Θ	5	k_{22}	-1
k_{11}	0.1	k_{23}	-5
k_{12}	-5	λ_Θ	0.2
k_{13}	-1	λ_ϖ	0.2
k_{21}	0.2		

The reference profiles for the attack angle and bank angle are designed for a cycle 8 task [14]. The model parameters are selected randomly within a ±20% range around their nominal values. The simulation results are shown in Figs. 1-4.

Figure 1 shows the attack angle tracking results. It can be seen from the top part that the actual attack angle almost coincides with its command profile, and from the bottom part that the attack angle tracking error is smaller than 0.04 deg throughout the simulation.

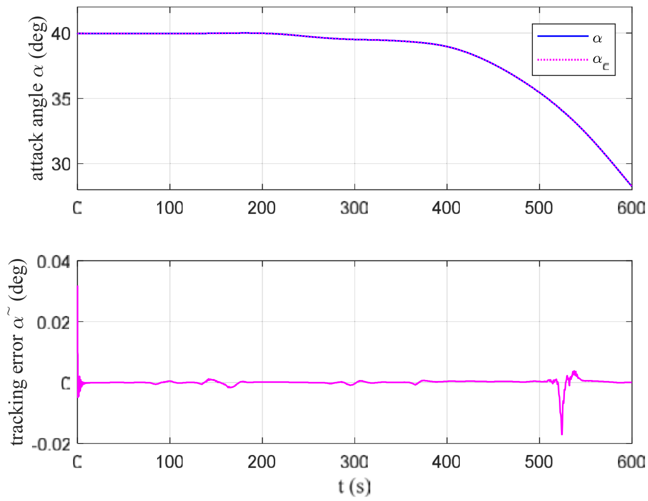

Fig. 1: Curves of the attack angle and its tracking error

Figure 2 shows the bank angle tracking results. It can be seen from the top part that the actual bank angle is nearly the same as its command profile, and from the bottom part that the bank angle tracking error keeps within about 2 deg.

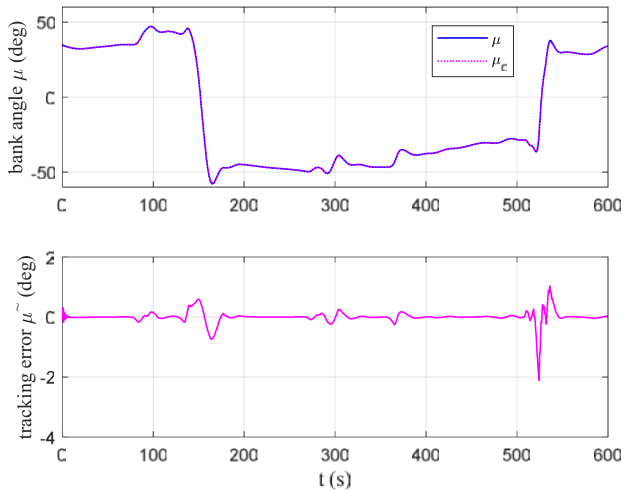

Fig. 2: Curves of the bank angle and its tracking error

Figure 3 shows the bank angle tracking result. It can be observed that the bank angle maintains in a small region around zero and is bounded by [-0.6, 0.4] deg, so that the system will not overheat during the reentry.

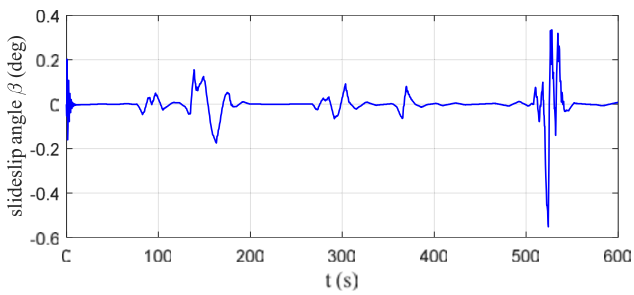

Fig. 3: Curves of the sideslip angle

Figure 4 shows the curves of the two control inputs, both of which are bounded and change smoothly.

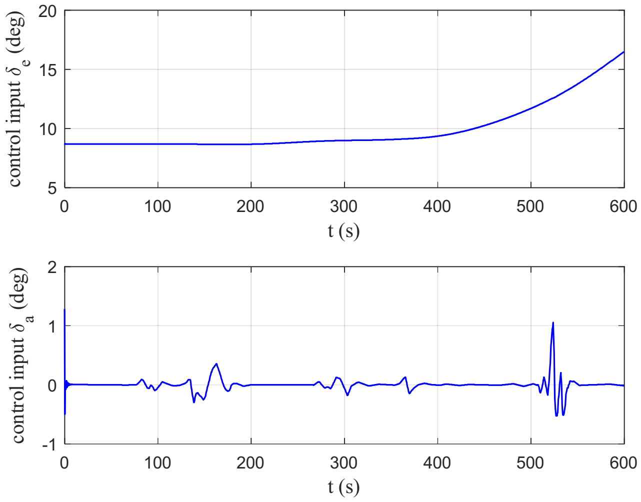

Fig. 4: Curves of the two control inputs

Therefore, the simulation demonstrates that the proposed controller has successfully stabilized the overall system and realized the control goal.

5 Conclusion

Reusable launch vehicles (RLVs) may experience underactuation and exhibit nonminimum phase problem during the middle phase of reentry, which will lead to failure of the traditional methods which are designed for a fully actuated RLV. In this paper, an approach combining backstepping and partial feedback linearization is proposed to address this issue. A modification is made on the inner loop design of backstepping by using partial feedback linearization to linearize the system to the maximum extent and locally stabilize the nonlinear part at the same time. Besides, a disturbance observer is designed for each loop to compensate the lumped uncertainties. It is shown that the proposed method successfully stabilizes the overall system as well as achieve the control goal only with limited numbers of control inputs. This approach is very effective for underactuated systems which is not in an integral chain form and may be applied to other underactuated systems in the future.

References

[1] B. Tian, Q. Zong, J. Wang, et al., Quasi-Continuous High-Order Sliding Mode Controller Design for Reusable Launch Vehicles in Reentry Phase, *Aerospace Science and Technology*, 28 (1): 198-207, 2013.

[2] J. Geng, Y. Sheng, X. Liu, Finite-Time Sliding Mode Attitude Control for a Reentry Vehicle with Blended Aerodynamic Surfaces and a Reaction Control System, *Chinese Journal of Aeronautics*, 27 (4): 964-976, 2014.

[3] Q. Dong, Q. Zong, B. Tian, et al., Adaptive-Gain Multivariable Super-Twisting Sliding Mode Control for Reentry RLV with Torque Perturbation, *International Journal of Robust and Nonlinear Control*, 27(4): 620-638, 2017.

[4] F. Wang, Q. Zong, B. Tian, Adaptive Backstepping Finite Time Attitude Control of Reentry RLV with Input Constraint, *Mathematical Problems in Engineering*, 2014: 1-19.

[5] F. Wang, C. Hua, Q. Zong, Attitude Control of Reusable Launch Vehicle in Reentry Phase with Input Constraint via Robust Adaptive Backstepping Control, *International*

Journal of Adaptive Control and Signal Processing, 29(10): 1308-1327, 2015.

[6] Z. Wang, Z. Wu, Y. Du, Robust Adaptive Backstepping Control for Reentry Reusable Launch Vehicles, *Acta Astronautica*, 126(1): 258-264, 2016.

[7] C. E. Hall, Y. B. Shtessel, Sliding Mode Disturbance Observer-Based Control for a Reusable Launch Vehicle, *Journal of Guidance, Control, and Dynamics*, 29(6): 1315-1328, 2006.

[8] B. Tian, L. Yin, H. Wang, Finite-Time Reentry Attitude Control Based on Adaptive Multivariable Disturbance Compensation, *IEEE Transactions on Industrial Electronics*, 62(9): 5889-5898, 2015.

[9] R. Su, Q. Zong, B. Tian, M. You, Comprehensive Design of Disturbance Observer and Non-Singular Terminal Sliding Mode Control For Reusable Launch Vehicles, *IET Control Theory & Applications*, 9(12): 1821-1830, 2015.

[10] Q. Mao, L. Dou, Q. Zong, et al., Attitude Controller Design for Reusable Launch Vehicles During Reentry Phase via Compound Adaptive Fuzzy H-Infinity Control, *Aerospace Science and Technology*, 72, (1): 36-48, 2018.

[11] G. Ma, C. Chen, Y. Lyu, et al., Adaptive Backstepping-Based Neural Network Control for Hypersonic Reentry Vehicle with Input Constraints, *IEEE Access*, 6(1): 1954-1966, 2018.

[12] R. R. Da Costa, Q. P. Chu, J. A. Mulder, Reentry Flight Controller Design Using Nonlinear Dynamic Inversion, *Journal of Spacecraft and Rockets*, 40 (1): 64-71, 2003.

[13] W. R. Van Soest, Q. P. Chu, et al., Combined Feedback Linearization and Constrained Model Predictive Control for Entry Flight, *Journal of Guidance, Control, and Dynamics*, 29 (2): 427-434, 2006.

[14] E. M. Wallner, K. H. Well, Attitude Control of a Reentry Vehicle with Internal Dynamics, *Journal of Guidance, Control, and Dynamics*, 26(6): 846-854, 2003.

[15] Z. Wang, W. Bao, H. Li, Second-Order Dynamic Sliding-Mode Control for Nonminimum Phase Underactuated Hypersonic Vehicles, *IEEE Transactions on Industrial Electronics*, 64(4): 3105-3112, 2017.

[16] W. Nie, H. Li, R. Zhang, Observer-Based Attitude Controller for Lifting Re-Entry Vehicle with Non-Minimum Phase Property, *International Journal of Advanced Robotic Systems*, 14(3): 1-13, 2017.

[17] G. Piovan, K. Byl, Approximation and control of the slip model dynamics via partial feedback linearization and two-element leg actuation strategy, *IEEE Transactions on Robotics*, 32(2): 399-412, 2016.

[18] A. Le, S. G. Lee, S. C. Moon, Partial feedback linearization and sliding mode techniques for 2D crane control, *Transactions of the Institute of Measurement and Control*, 36(1): 78-87, 2014.

[19] M. A. Mahmud, H. R. Pota, M. J. Hossain, et al., Robust partial feedback linearizing stabilization scheme for three-phase grid-connected photovoltaic systems, *IEEE Journal of photovoltaics*, 4(1): 423-431, 2014.

[20] H. K. Khalil, *Nonlinear systems*, 1st edn., Prentice-Hall, 1996.